

CW Performance of an InGaAs-GaAs-AlGaAs Laterally-Coupled Distributed Feedback (LC-DFB) Ridge Laser Diode

R.D. Martin, S. Forouhar, S. Kco, R.J. Lang, R.G. Hunsperger, R.C. Tiberio, and P.F. Chapman.

Abstract – Single-mode distributed feedback (DFB) laser diodes typically require a two-step epitaxial growth or use of a corrugated substrate. We demonstrate InGaAs-GaAs-AlGaAs DFB lasers fabricated from a single epitaxial growth using lateral evanescent coupling of the optical field to a surface grating etched along the sides of the ridge. A CW threshold current of 25 mA and external quantum efficiency of 0.48 mW/mA per facet were measured for a 1 mm cavity length device with anti-reflection coated facets. Single-mode output powers as high as 11 mW per facet at 935 nm wavelength were attained. A coupling coefficient of at least 5.8 cm^{-1} was calculated from the subthreshold spectrum taking into account the 2 % residual facet reflectivity.

R.D. Martin and R.G. Hunsperger are with the Department of Electrical Engineering, University of Delaware, Newark, Delaware 19716

S. Forouhar and S. Kco are with the Center for Space Microelectronics Technology, Jet Propulsion Laboratory, California Institute of Technology, 4800 Oak Grove Drive, Pasadena, California 91109

R.J. Lang was with the Center for Space Microelectronics Technology, Jet Propulsion Laboratory. He is now with SDL, inc., 80 Rose Orchard Way, San Jose, California 95134

R. Tiberio and P. Chapman are with the National Nanofabrication Facility, Cornell University, Ithaca, New York 14853

CW Performance of an InGaAs-GaAs-AlGaAs Laterally-Coupled Distributed Feedback (LC-DFB) Ridge Laser Diode

R.D. Martin, S. Forouhar, S. Kco, R.J. Lang, R.G. Hunsperger, R.C. Tiberio, and P.F. Chapman.

I. INTRODUCTION

Stable single longitudinal mode behavior, narrow linewidths (\sim MHz), low power requirements, and small size have made distributed feedback (DFB) semiconductor laser diodes attractive in many applications including, spectroscopy, pump sources for amplifiers, injection sources for solid-state lasers, and as both sources and local oscillators in coherent communication systems. DFB laser diodes achieve wavelength selectivity by incorporating a periodic change of refractive index or gain along the lasing cavity. This is usually done by growing the laser structure on a corrugated substrate or by interrupting the growth above the active region, patterning and etching the grating, and then growing the upper cladding and cap layers. Determining the proper surface preparation and growth parameters to achieve high quality epitaxial regrowth while preserving the grating structure is technically demanding - particularly for short wavelength AlGaAs lasers with high aluminum content and long wavelength GaSb based devices.

One way to eliminate the regrowth problem is to rely on evanescent coupling of the electromagnetic fields to a surface grating. This approach has been demonstrated by etching the grating directly over the waveguide and injecting the current from the side [1] or by etching the grating through the cap and upper cladding layer to provide the lateral index guiding for the 'ridge' and selective feedback [2]. Both of these techniques require a deep, uniform transfer of the grating into the upper cladding. An alternative approach is to etch the ridge first and then define the grating on either side of the ridge (Fig. 1) by either electron beam [3-4] or x-ray [5] lithography. The difficulty with this structure lies in achieving sufficient interaction of the evanescent field with the surface grating. Agrawal and Dutta have shown that the threshold of a ridge DFB increases by a factor of 20 or more when the gratings under the ridge are removed [6]. In this Letter the CW lasing characteristics of a laterally-coupled distributed feedback (LC-DFB) ridge laser using a single growth step are presented.

11. FABRICATION

The fabrication of LC-DFB lasers is very similar to that of standard ridge lasers. Photolithography was used to define 2 μm wide photoresist stripes on an MBE grown InGaAs-GaAs-AlGaAs graded index separate confinement heterostructure (GRINSC11). Chemically assisted ion beam etching (CAIBE) using chlorine gas in conjunction with an argon ion beam was used to etch the ridges 10 within $(\pm) 0.1 \mu\text{m}$ of the GRINSC11. The two dimensional overlap of the electric field with the grating - and hence the coupling coefficient, κ - is critically dependent on the ridge etch depth and width [7]. Etching the ridge too deep results in strong index guiding of the field and reduces the lateral (y - direction) fill factor of the grating. Too shallow of a ridge depth reduces the transverse (x - direction) overlap of the field with the grating. A narrow ridge was used to increase the lateral overlap of the electric field with the grating.

After etching the ridge, PMMA was applied to the wafer and a first order grating was exposed (Fig. 2) using electron beam lithography. To simplify alignment of the e-beam pattern to the ridge, the grating was written continuously across the structure. Grating free ridges were included in the pattern to permit comparison of Fabry-Perot and DFB devices from the same wafer. CAIBE was then used to transfer the grating approximately 700 \AA deep into the cap layer and upper cladding beside the ridge. The grating depth was much less than the thickness of the highly doped cap region. The high resolution e-beam configuration used to expose the grating pattern resulted in very narrow exposed lines ($\sim 25 \text{ nm}$) yielding an etched to unetched aspect ratio of 1:5 (16.6 % duty cycle) for the etched grating. For a rectangular shaped first order grating, optimal feedback is achieved with a symmetric grating - i.e., a 50% duty cycle. A self-aligning technique using silicon nitride and polyimide was used to planarize the wafer and facilitate contacting the narrow ridge. The wafer was thinned and finished with Cr/Au (p-type) and AuGe/Ni/Au (n-type) contacts. Devices were mounted junction side up on copper heat sinks for testing. Anti-reflection coatings consisting of a quarter wavelength ($\lambda/4$) of Al_2O_3 (R - 2 %) were deposited on both facets of the DFB devices to suppress Fabry-Perot modes.

11.1. MEASUREMENT'S AND ANALYSIS

Laterally-coupled DFB lasers with cavity lengths of 1.0 and 1.5 mm had as-cleaved CW threshold currents of 10 - 15 mA which increased to 18-25 mA when AR coated. Power-current ($P-I$) characteristics of a 1.0 mm cavity length LC-DFB laser with AR coatings are shown in figure 3. The threshold current and

external slope efficiency are 25 mA and 0.48 mW/mA per facet. LC-DFB devices with cavity lengths of 250 μm to 500 μm had CW threshold currents of 8 - 10 mA with as-cleaved facets. When AR coated, however, threshold currents increased to 35 - 80 mA indicating insufficient grating feedback (i.e. weak coupling) for these cavity lengths.

The inset of figure 3 shows the CW spectral characteristics of a 1 mm device measured with a 3/4 m spectrometer as the current is increased from 30 - 45 mA in 5 mA steps. Single-mode DFB operation was observed up to 11 mW at which point a second DFB mode begins to lase. The side-mode suppression ratio (SMSR) measured with an optical spectrum analyzer was greater than 30 dB at an output power of 10 mW. The lasing wavelength as a function of heat sink temperature was measured for a LC-DFB laser along with a standard ridge laser. The lasing wavelength of the ridge devices without gratings shifted at $-3 \text{ \AA}/^\circ\text{C}$ compared to a much slower rate of $0.65 \text{ \AA}/^\circ\text{C}$ for the LC-DFB devices.

The coupling coefficient can be determined from the subthreshold normalized stop-band width [8], WL , defined as the normalized mode spacing between the fundamental (lowest threshold) DFB mode and the lowest threshold adjacent DFB mode, i.e.,

$$WL = 2\pi n_{eff} L \left| \frac{1}{\lambda} - \frac{1}{\lambda_{\pm}} \right| = 2\pi n_{eff} L \frac{\Delta\lambda}{\lambda^2} \quad (1)$$

In this equation λ , λ_{-} , and λ_{+} are the wavelengths of the fundamental, shorter adjacent, and longer adjacent modes, n_{eff} is the effective index including the dispersion [9], and L is the laser cavity length. The relationship between WL and κL is shown in figure 4 for the case of 0 % and 2 % facet reflectivity. The perfect AR case is calculated using the theory of Kogelnik and Shank [10]. It becomes more difficult to determine the coupling when the residual facet reflectivity is taken into account because the phase of the grating at the front and rear facets is unknown. For the 2 % case, the phases of the grating at the front and rear facets were each varied from 0 to $15 \pi/8$ in $\pi/8$ steps. The normalized threshold gain (αL) and frequency deviation from the Bragg condition (δL) of the 5 modes nearest the Bragg wavelength were calculated [11] for each of the 256 phase combinations for κL values ranging from 0.2 to 1.0. The minimum and maximum normalized stop-band width were extracted for each κL value. Figure 4 shows that for a given value of κL , the residual reflectivity and random grating phase of the facets introduces a large variation in the stop-band width. WL values of 4.14 ($L = 1.0 \text{ mm}$) and 4.61 ($L = 1.5 \text{ mm}$) were measured on subthreshold spectra of LC-DFB lasers. Figure 4 shows that for the measured WL values, κL is at least 0.59 ($\kappa = 5.9 \text{ cm}^{-1}$)

and 0.87 ($\kappa = 5.8 \text{ cm}^{-1}$) for the 1 mm and 1.5 mm devices respectively. In general, for good performance of a DFB laser, a κL product of 1 - 1.5 is desired. A theoretical coupling coefficient of 8.6 cm^{-1} was determined by applying coupled-mode theory [7] to the InGaAs LC-DFB laser with a 16.6% duty cycle rectangular grating. This analysis revealed that the coupling coefficient would be doubled with a 50% duty cycle grating. If the minimum measured coupling value ($\kappa = 5.8 \text{ cm}^{-1}$) is doubled by using a symmetric grating, a κL of 1.0 could be attained for a LC-DFB laser with a 900 nm cavity length.

IV. SUMMARY AND CONCLUSION

Single mode distributed feedback laser diodes were produced from a single epitaxial growth that rely on the lateral coupling of the evanescent electromagnetic fields with a surface grating etched along the sides of the ridge. Good performance of strained layer InGaAs-GaAs-AlGaAs SQW LC-DFB lasers was achieved. A 25 mA CW threshold current, total external quantum efficiency of 82%, and single longitudinal mode output power of 11 mW were attained for a 1 mm cavity length laterally-coupled device. The 2 % residual facet reflectivity of the anti-reflection coating used on the LC-DFB lasers prevented an exact measurement of κ from the stop-band but taking into account the random phase of the grating at the facets, a minimum coupling coefficient of 5.8 cm^{-1} was determined from the subthreshold spectra. We have demonstrated that a laterally-coupled DFB laser has potential as a stable, single-mode device with power levels suitable for many applications. This technique could be used to fabricate DFB lasers in material systems for which regrowth is prohibitive - such as high Al concentration (short wavelength and visible lasers) and GaSb (long wavelength) based devices.

ACKNOWLEDGMENTS

The work described in this Letter was performed in part at the Center for Space Microelectronics Technology, Jet Propulsion Laboratory, California Institute of Technology and was sponsored by the Ballistic Missile Defense Organization, Innovative Science and Technology Office and in part at the National Nanofabrication Facility which is supported by the National Science Foundation under Grant ECS-8619049, Cornell University and industrial affiliates. R. Martin has been supported through a NASA Graduate Student Research Fellowship.

REFERENCES

- [1] Z. I. Liao, D.C. Flanders, J.N. Walpole, and N.L. DeMeo, "A novel GaInAsP/InP distributed feedback laser," *Applied Physics Letters*, Vol. 46, No. 3, pp. 221-223, 1 Feb. 1985.
- [2] L.M. Miller, K.J. Beernink, J.T. Verdeyen, J.J. Coleman, J.S. Hughes, G.M. Smith, J. I. Ionig, and T.M. Cockerill, "Characterization of an InGaAs-GaAs-AlGaAs Strained-Layer Distributed-Feedback Ridge-Waveguide Quantum-Well Heterostructure Laser," *IEEE Photonics Technology Letters*, Vol. 4, No. 4, pp. 296-299, April 1992.
- [3] R. H. Martin, S.F. Forouhar, S. Keo, R.J. Lang, R.G. Hunsperger, R.C. Tiberio, and P.F. Chapman, "InGaAs-GaAs-AlGaAs Laterally-Coupled Distributed Feedback (LC-DFB) Ridge Laser Diode", *Electronics Letters*, Vol. 30, No. 13, pp. 1058-1060, 23 June 1994.
- [4] R.C. Tiberio, P.F. Chapman, R.D. Marlin, S.F. Forouhar, and R.J. Lang, "Laterally Coupled Distributed Feedback Lasers Fabricated with Electron Beam Lithography and Chemically Assisted Ion Beam Etching," to be published in the *Journal of Vacuum Science and Technology B*.
- [5] V.V. Wong, W. Choi, J. Carter, C.G. Fonstad, and H.I. Smith, "Ridge-Grating Distributed-Feedback Lasers Fabricated by X-Ray Lithography," *Journal of Vacuum Science and Technology B*, Vol. 11, p. 2621, 1993.
- [6] G.P. Agrawal and N.K. Dutta, "Analysis of Ridge-Waveguide Distributed Feedback Lasers," *IEEE Journal of Quantum Electronics*, Vol. QE-21, No. 6, pp. 534-538, June 1985.
- [7] R.D. Martin, S. Forouhar, R.J. Lang, and R.G. Hunsperger, unpublished.
- [8] K. Kihara, H. Soda, H. Ishikawa, and H. Imai, "Evaluation of the coupling coefficient of a distributed feedback laser with residual facet reflectivity," *Journal of Applied Physics*, Vol. 62, No. 4, pp. 1526-1527, 15 August 1987.

- [9] K. Iga, "On the use of the effective refractive index in DFB laser mode separation," *Japanese Journal of Applied Physics*, Vol. 22, No. 1(), p. 1630, 1983.
- [10] H. Kogelnik and C.V. Shank, "Coupled-Wave theory of Distributed Feedback Lasers," *Journal of Applied Physics*, Vol. 43, No. 5, pp. 2327-2335, May 1972.
- [11] W. Streifer, R. D. Burnham, and D. R. Scifres, "Effect of external reflectors on longitudinal modes of distributed feedback lasers," *IEEE Journal of Quantum Electronics*, Vol. QE-11, No. 4, pp. 154-161, April 1975.

LIST OF FIGURES

Fig. 1 Diagram of a laterally-coupled distributed feedback (LC-DFB)ridge laser diode.

Fig. 2 Scanning electron micrograph of the first order grating pattern over the ridge defined in PMMA by-beam lithography.

Fig. 3 CW power-current and spectral characteristics of a 1 mm cavity LC-DFB laser with AR coated facets. For the spectral data the current is stepped from 30 mA to 45 mA in 5 mA steps.

Fig. 4 Relationship between the normalized stop-band width, WL , and κL for residual facet reflectivity of 0 % and 2 %. For the 2 % case, the phases of the grating at each facet were varied from 0 to $15\pi/8$ in $\pi/8$ steps. The minimum and maximum normalized stop-band width obtained from the 256 phase combinations are shown.

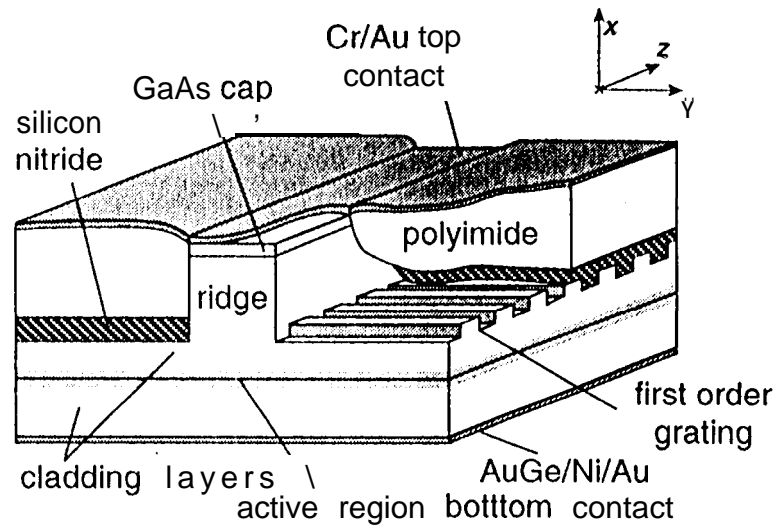


Fig. 1 Diagram of a laterally-coupled distributed feedback (LC-DFB) ridge laser diode,



Fig. 2 Scanning electron micrograph of the first order grating pattern over the ridge defined in PMMA by e-beam lithography.

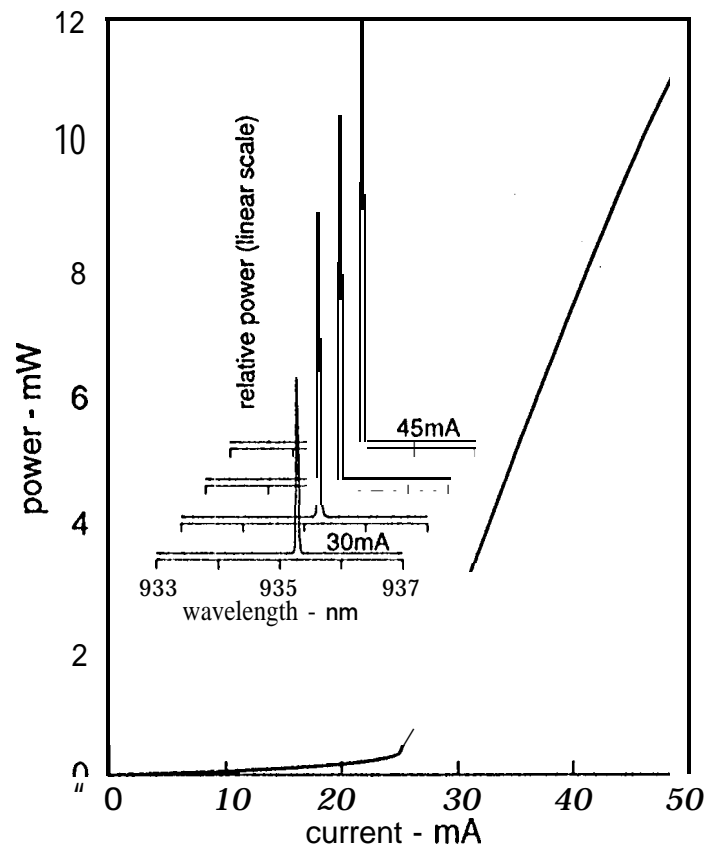


Fig. 3 CW power-current and spectral characteristics of a 1 mm cavity LC-DFB laser with AR coated facets. For the spectral data the current is stepped from 30 mA to 45 mA in 5 mA steps.

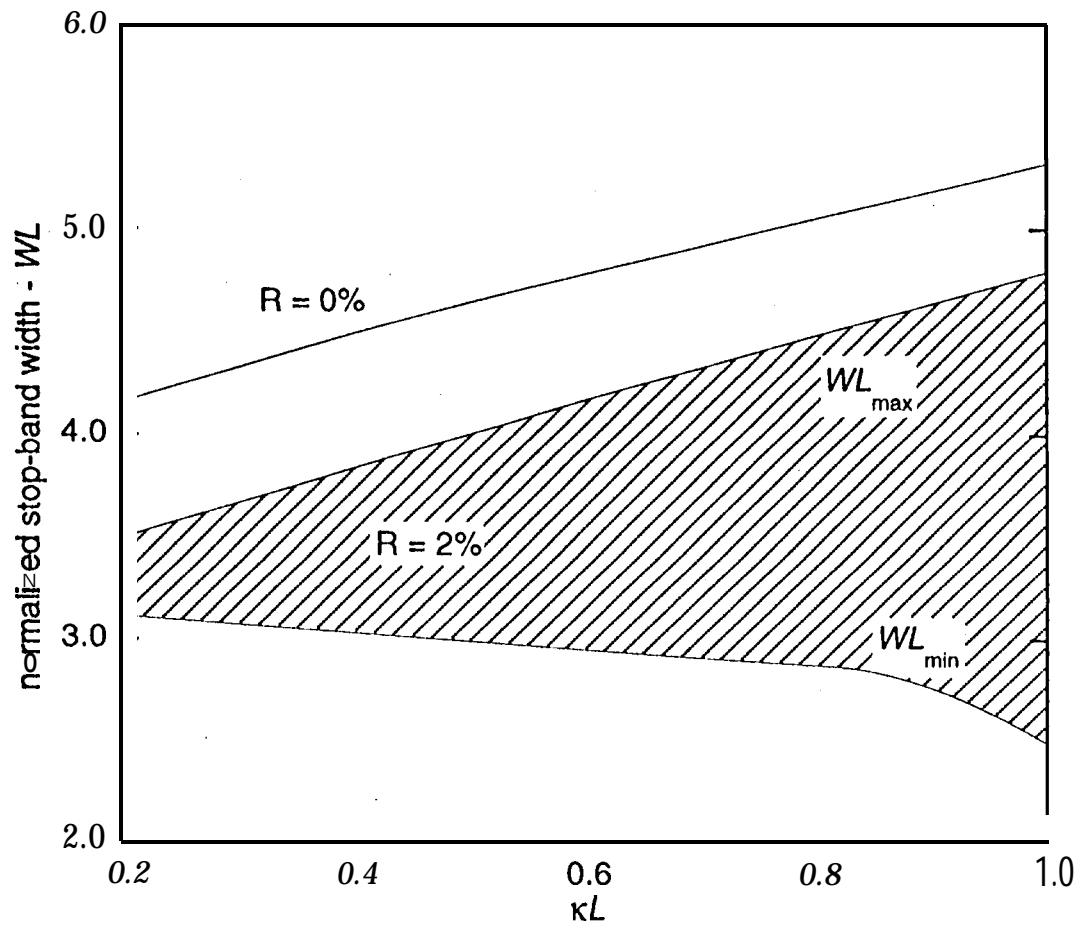


Fig. 4 Relationship between the normalized stop-band width, WL , and κL for residual facet reflectivity of 0.% and 2 %. For the 2 % case, the phase of the grating at both facets was varied from 0 to $15\pi/8$ in $\pi/8$ steps. The minimum and maximum normalized stop-band width obtained from the 256 phase combinations are shown.